High resolution MLC leaf position measurements with a large area MAPS

J. L. Pritchard, J. J. Velthuis, L. Beck, C. De Sio, R. P. Hugtenburg

***Abstract*—Multileaf collimators (MLC) are an essential component in modern radiotherapy that shape the X-ray treatment beam. Currently, MLC leaf position accuracy is verified to $\pm$1 mm every month. However, leaf position accuracy can drift between verification dates and treatment verification only occurs pre-treatment. To prevent serious errors, it would be highly beneficial to use a real time verification system. We are developing a system based on Monolithic Active Pixel Sensors (MAPS). MAPS are radiation hard under photon and electron irradiation, have high readout rates, low attenuation and are suitable for high resolution applications making them an ideal upstream radiation detector. Here, we report results using the Lassena MAPS, which measures 12$\times$14 cm^2 and is three side buttable, allowing full treatment fields to be monitored. The Lassena detector was placed in the treatment field of an Elekta Synergy LINAC which has an MLC leaf width of 0.5 cm. An MLC leaf was extended to 10 different positions within the field. Sobel based methods were used to reconstruct the leaf edge position. Correspondence between reconstructed and set leaf position was excellent and resolutions ranged between 60.6$\pm$8 μm and 109$\pm$12 μm for a central leaf with leaf extensions ranging from 1 to 35 mm using $\sim$0.3 s of treatment beam time while the sensor was placed at an SSD of 85 cm.**

***Index Terms*—Edge finding, Monolithic Active Pixel Sensors (MAPS), Multileaf Collimators (MLC), Radiotherapy, Real time verification.**

I. Introduction

According to Public Health England, in 2017 around half of all cancer patients in the United Kingdom had some form of radiotherapy included in their treatment management, which contributed to 40% of all cured cases [1]. The NHS and UK government have therefore stressed its importance and are pushing to increase the prevalence of advanced radiotherapies, such as Image Guided Radiotherapy (IGRT) and Intensity Modulated Radiotherapy (IMRT) which have been shown to further increase patient survival rates [2]. The multileaf collimator (MLC) plays a key role in the delivery of advanced therapies and hence significantly contributes to the increased rates of patient survival. An MLC is a collimation device situated in the linear accelerator (LINAC) head and shapes the treatment field prior to patient interaction. The device consists of two opposing rows of tungsten leaves, in which the individual leaves move independently of each other, allowing for complex static or dynamic radiotherapy treatment field shapes to be created during treatment delivery. Healthy tissue is therefore less irradiated while the therapeutic dose to malignant tissues can be increased [3].

To ensure that a patient receives the correct dose in the correct locations, precise MLC leaf edge positioning is of fundamental importance. MLC positions, however, are only verified on a monthly basis [4]. Standard verification methods use radiographic films or more recently an Electronic Portal Imaging Device (EPID) to image field configurations and manually adjust MLC positions accordingly. The Task Group 142 (TG-142) report, which sets international standards for quality assurance in radiotherapy, has therefore defined an acceptable static leaf position accuracy of 1 mm. Additionally, a dynamic IMRT field tolerance of 3.5 mm in terms of error counts is also specified [4]. Current MLC calibration methods have been shown to yield differences between leaf position readout and radiation field size ranging between 0.5 and 1.2 mm for each leaf bank [5]. In addition to modifying the spatial distribution of the delivered treatment plan, systematic offsets of $\pm$1 mm have been shown to alter the total prescribed dose by 2-4 % for bladder, rectum, brainstem, larynx, parotid and spinal cord treatments. More complex treatments, such as those used in IMRT which utilise small field sizes therefore have a higher sensitivity to systematic errors [6]. Individual MLC errors have also been shown to occur during treatment delivery. A study which analysed the log files of 91 IMRT treatment plans, showed that 80% of the 34212 treatment segments analysed contained at least one MLC leaf error which exceeded the set $\pm$1 mm tolerance [7]. Although individual MLC errors of $\pm$2 mm have a negligible effect on total treatment dose [6] [8], localised under/over radiation exposure can be of significance as the dose gradient at an MLC leaf edge can exceed 10% per mm. These large localised differences are therefore of clinical significance when considering critical, small structures or small treatment fields [5]. Furthermore, if an MLC leaf position exceeds $\pm$2 mm, an interlock will halt treatment delivery. However, slow moving leaves can become stuck if not replaced and random MLC errors are only identified in post-treatment reviews [9]. It has been suggested that in addition to correctly verifying MLC leaf edges, the verification tolerance should be set to a higher standard of $\pm$0.3 mm [6] [8], as this will maintain total dose errors below 2% for complex

J. L. Pritchard is with the School of Physics, University of Bristol, Bristol BS8 1TL, U.K., (e-mail: jordan.pritchard@bristol.ac.uk).

J. J. Velthuis is with the School of Physics, University of Bristol, Bristol BS8 1TL, U.K., also with Swansea University Medical School, Swansea SA2 8PP, U.K., and also the School of Nuclear Science and Technology, University of South China, Hengyang 421001, China.

L. Beck and C. De-Sio are with the School of Physics, University of Bristol, Bristol BS8 1TL, U.K.

R. P. Hugtenburg is with Swansea University Medical School, Swansea SA2 8PP, U.K., also with the Department of Medical Physics and Clinical Engineering, Abertawe Bro Morgannwg University Hospital Board, Swansea SA2 4QA, U.K., and also with the School of Physics, University of Bristol, Bristol BS8 1TL, U.K.

Manuscript received (Month?) (day?), 2019; revised (Month?) (Day?), 2019.

treatments, in line with TG-142 [4].

In addition to monthly MLC verification, pre-treatment verification is also recommended for each treatment. Currently, standard verification methods consist of delivering the prescribed treatment plan to a phantom, containing in-vivo ion chamber(s) and radiographic film(s) or an EPID prior to patient delivery [4]. MLC configurations and deposited dose are checked, increasing the total LINAC usage time, so pre-treatment verification is often not performed for each individual treatment, but instead for an acceptable sample of patients and/or treatment fractions. Incorporating a high precision, real time treatment monitoring device would allow systematic and random MLC errors to be identified instantaneously and subsequently addressed. The need for pre-treatment verification would also be eliminated as each treatment would be verified in real time. Patient throughput, safety, treatment quality and effectiveness would therefore be increased.

II. Current Treatment Verification Devices

Radiotherapy verification devices exist and are categorised into upstream and downstream detectors. Upstream detectors are placed between the radiotherapy source and patient, examples of which include DAVID [11] and COMPASS [12] devices.

DAVID is attached to the LINAC head and consists of a flat plate ionisation chamber with readout wires under each MLC leaf edge, spaced 4.31 ± 0.1 mm apart with a 1s readout time. Devices are customised for each MLC type as a readout wire must be present under each leaf. To detect the MLC position and hence any positioning error, the signal intensity produced in each wire during radiation is compared to a reference value obtained from daily dark data. Leaf edge errors of ±1 mm can therefore be identified. COMPASS is composed of a 2D array of 1600 parallel plate ionisation chambers, which is also attached to the LINAC head. Segments are 3.8 mm in diameter and spaced 6.5 mm apart with a 20 ms sample rate. This detector is primarily used for dose verification pre or post treatment. It has been used to validate treatment deliveries by gamma analysis, in which delivered and planned treatments are compared. As both of these detectors are composed of ionisation chambers, thick build-up material is required to generate enough ionisation events to create a measurable signal. The therapeutic treatment beam is therefore attenuated by 3.3% and 4-5% for the DAVID and COMPASS devices respectively [11] [12]. Additionally, secondary electrons are also produced which irradiates tissue outside the planned treatment volume and increases surface dose. Alternatively, downstream detectors such as EPIDs can be placed behind the patient. Generally, EPID refers to any electronic device placed downstream of the patient which produces image data for analysis. Examples include phosphor plate and digital camera combinations, various ion chamber configurations and silicon array detectors. Across all types of EPID, when tested with no patient present, best MLC leaf edge precisions have been shown to vary between ±0.6 and 0.3 mm [13]. Precisions of 0.1 mm have been achieved with the iViewGT, which is a flat silicon array detector, 41×41 cm^2 in size, with a 1024×1024 pixel array yielding a pixel pitch of 0.25 mm at isocentre. However, to achieve 0.1 mm precisions, additional radiographic film measurements and multiple correction factors are required [14]. As such, total data acquisition time can take up to 20 mins. EPID systems can therefore provide precise measurements for verification pre or post treatment. However, such precision measurements are not possible during live treatment. Additionally, during treatment delivery, the patient is situated between the X-ray source and detector. The patients volume and non-uniform anatomy creates significant and non-uniform attenuation of the treatment beam. Considerable scatter components are also introduced. The best precision of MLC leaf edge measurements will therefore be diminished irrespective of downstream detector type.

III. Monolithic Active Pixel Sensors

In this work, MLC leaf positions are detected by a monolithic active pixel sensor (MAPS) placed at a position that would be upstream of a patient in an eventual clinical implementation. Using MAPS to detect leaf positions was first pioneered by us [15] and subsequently patented [16] [17]. MAPS are produced by growing a lightly p doped epitaxial layer on top of a heavily p doped substrate. Next the top is again heavily p doped. In this top layer n-type collection diodes are made, see Fig. 1, and the first readout stage is implemented. The MAPS used in this work has a so-called 3T architecture; each pixel cell has a reset transistor, a source follower and a select switch, see Fig. 2. The sensor is front illuminated, i.e. the treatment beam first traverses the epi layer before entering the bulk. During irradiation, ionisation events occur in the epitaxial layer and mobile charge carriers are generated. Charge carriers will diffuse through the silicon via a random walk process. Due to the built in potentials, electrons are confined to the epitaxial layer and will be collected at the n-well. Holes will be swept into the p++ bulk. Collected charge subsequently builds up on the gate of the source follower and hence affects the drain current when the select switch is opened. Thus the measured current reflects the collected charge at the n-well. MAPS can be made very thin as the bulk layer is largely for support and hence can be thinned to a few microns, the sensitive layer can be 1–20 μm thick and the protective silicon dioxide layer a fraction of this. Total beam attenuation is therefore $< 1\%$ [18] and clinically insignificant [19] [20]. Pixel sizes can be made very small, ranging from a few microns to $\sim$ 0.1 mm. MAPs are therefore highly suitable for high resolution applications, such as MLC leaf edge tracking [21].

IV. Lassena MAPS

It has been shown using the Achilles MAPS [22] that MLC leaf edge positions can be monitored to a precision of 52 ± 4 μm for a single data frame, running at 40 frames per second (fps) for leaves of 1 cm width at the isocenter [19]. Furthermore, leaf deviations as small as 0.5 mm were detected and it was shown that the sensor is capable of leaf tracking in dynamic fields with leaf speeds of up to 3.5 cm/s in a 6 MV

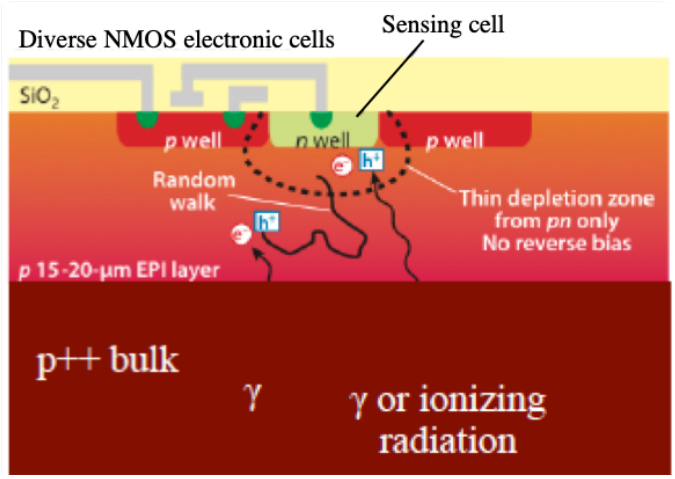

Fig. 1. Cross section diagram of a CMOS MAPS pixel showing the layer structure. Incident photons create ionisation events and hence electron-hole charge carriers, which subsequently perform a random walk. Electrons are collected at the n-well, as shown.

beam running at a dose-rate of approximately 600 MU/min [23]. A system using an Achilles MAPS has also been used to measure delivered dose for a Elekta LINAC at the University of Bristol Hospital Trust. It was shown that the dose could be precisely calculated, with 97% of dose distribution passing the 3% and ±3 mm gamma criteria [24]. This is more than good enough for clinical deployment. However, the Achilles MAPS is 5.7×5.7 cm^2 in size and has wire bonds on all sides. Hence, it is not possible to cover full treatment fields without big gaps.

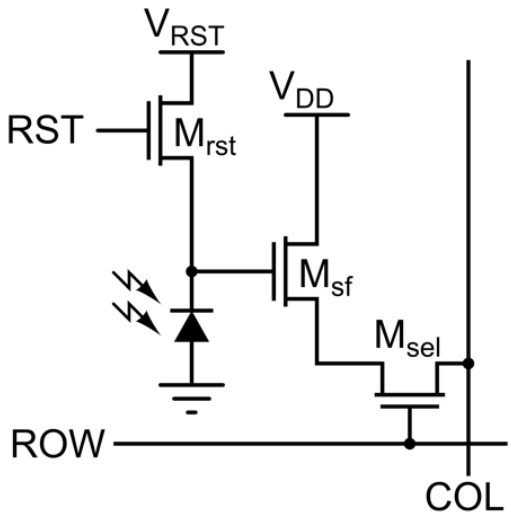

Fig. 2. Lassena 3T circuit diagram.

Large format MAPS are needed for the clinical implementation of leaf monitoring, where multiple and elongated treatment targets are the norm. Covering a full clinical field will require a detector with a cross-sectional area of around 25×25 cm^2 when installed at the LINAC head. Lassena, see Fig. 3, is a wafer scale CMOS image sensor intended for use in medical X-Ray imaging. It was designed in a 180 nm, dual

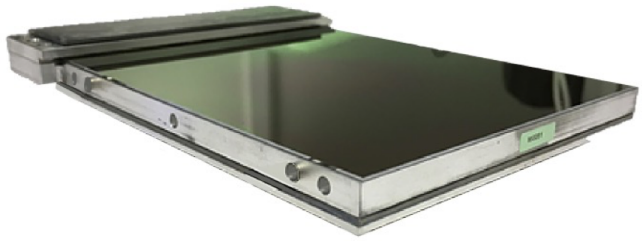

Fig. 3. Lassena MAPS sitting on a metal support frame. It should be noted that this frame is only present for the purpose of handling and is only situated around the sensor perimeter, hence the treatment beam is not affected by the frame during testing.

oxide, 5 metal, 1 poly CMOS Image Sensor process. Thick oxide transistors were used to maximise the dynamic range. The sensor measures 12×14 cm^2, has a 3T pixel architecture and a 50 μm pixel pitch [25]. Enclosed layout transistors were used throughout the sensor to ensure radiation tolerance. The sensor was designed to be 3-side buttable, hence a combined imaging area of 28 cm in one direction and any multiple of 12 cm in the other is achievable. A 2×2 configuration of Lassenas can therefore monitor full treatment fields and is hence clinically deployable. The sensor used in this experiment is 700 μm thick but can be thinned to well below 100 μm. It is readout through 32 analogue amplifiers working at 10 Mpixel/sec. When operating with standard settings, the maximum readout rate is 34 fps.

V. Experimental Setup

To determine the MLC leaf edge resolution at different positions in a treatment beam, the Lassena detector was placed on a 160 leaf Elekta Synergy LINAC treatment couch inside a light-tight environment. The detectors SSD in this work was 85 cm, with the intended position for clinical use being at the shadow tray which is approximately 55 cm SSD. Dark data frames were measured. A 5×5 cm^2 fixed field was selected and a single, central MLC leaf extended to a fixed position to collimate a 6 MV treatment beam. All surrounding leaves were held in a fixed position. Data was then recorded at 34 fps. This was repeated using the same central leaf at 10 different extensions throughout the field. Positional measurements are quoted for the isocenter.

VI. Leaf Edge Reconstruction & Resolution Methodology

Leaf positions are reconstructed following the method detailed in [19]. The signal of every pixel consists of a dark value, the pedestal, the beam induced signal and noise. To determine the pedestal for a pixel, the average signal for each pixel without beam was determined. The noise was subsequently determined as the standard deviation of the pixel output without beam present. Pixels whose pedestal and/or noise values were extremely different were excluded from further analysis. For this sensor, 12 pixels were excluded from the 1×10^6 pixel region of interest. The output of these 12 pixels was set to the average output of their surrounding 8

pixels. To reduce the high frequency noise, the image was smoothed using a Gaussian smearing with a radius of 31 pixels and a sigma of 7.

This procedure is followed for the Lassena after summing the data of 10 raw frames to reduce the random fluctuations between pixels. This effectively reduces the frame rate to 3.4 fps. Fig. 4 shows such a frame. The leaf is clearly visible. A one dimensional projection along the line y = 1150, i.e. through the leaf, can be seen in Fig. 5. The results, after following the procedure outlined above can be seen in Fig. 6 and Fig. 7, which indeed are a lot smoother. Applying a 3×3 Sobel operator, which is a discrete differential operator, results in Fig. 8. The leaf edge position is extracted as the location with the highest gradient in intensity as the leaves will block the photon beam. This is determined for each pixel row. Results are shown in Fig. 9. The final leaf position value is extracted by fitting the leaf position obtained for each pixel row with a parabola. The minimum of the parabola is used as the final leaf position.

The above described methodology is repeated for multiple frames. These measurements are plotted in a histogram, see Fig. 10. A Gaussian fit is then applied to the distribution and the sigma of the Gaussian is defined as the leaf edge position resolution.

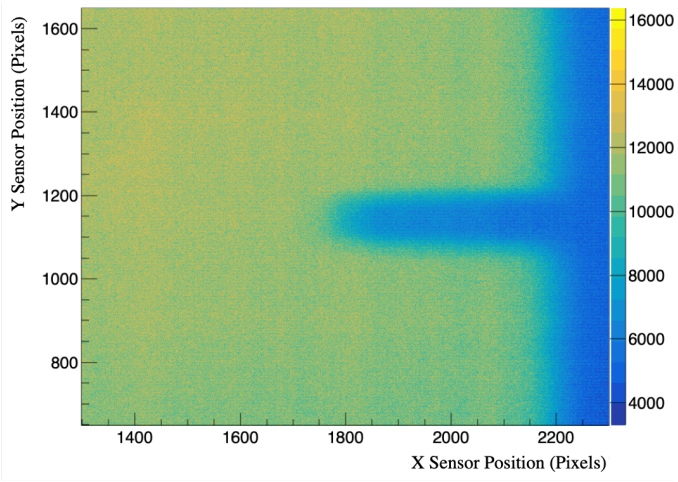

Fig. 4. Subsection of a data frame taken at 20mm extension in a radiotherapy treatment field using the Lassena. X and Y Sensor Positions are parallel and perpendicular to the direction of leaf travel respectively.

VII. Leaf Position Resolution

The procedure was repeated for 10 extensions ranging from 35 mm down to 1 mm. Fig. 11 shows the resolution for leaf extensions between 1 and 35 mm. Resolution values ranged between 60.6±7.65 μm and 109±12.3 μm at the isocentre, which shows that excellent resolution is achieved throughout the treatment field. This is much lower than the current MLC verification standard of ±1 mm and the recommended verification standard of ±0.3 mm previously described. Additionally, since each individual data point was obtained using 10 summed raw frames, which corresponds to ∼0.3 s of continuous data, it has been shown that good resolution can be

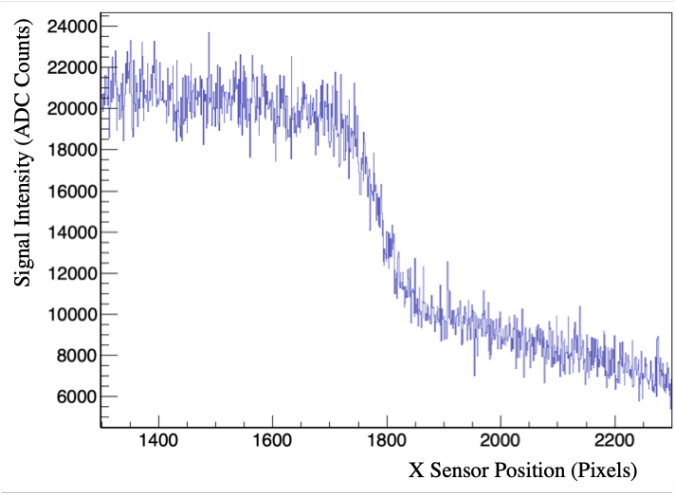

Fig. 5. Projection through the MLC leaf edge, at line 1150. High pixel-to-pixel intensity variations are observable.

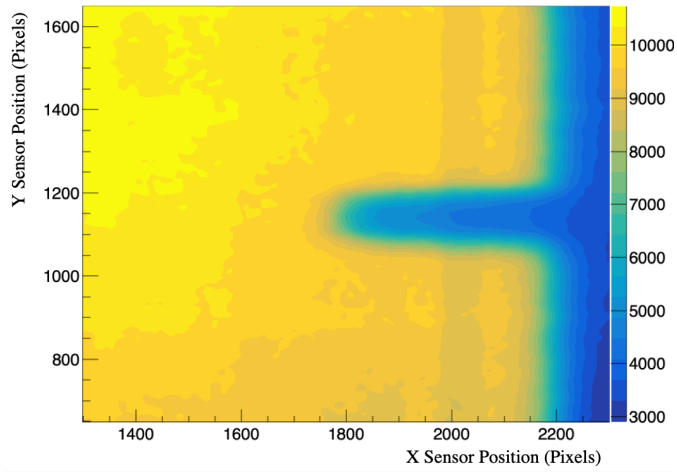

Fig. 6. Subsection of a data frame taken at 20mm extension after pedestal subtraction, bad pixel mask, and Gaussian smoothing.

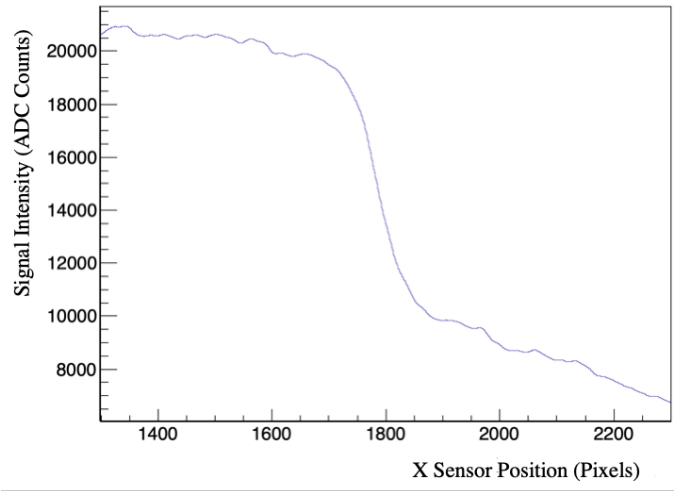

Fig. 7. Projection through the MLC leaf edge, after pedestal subtraction, bad pixel mask and Gaussian smoothing.

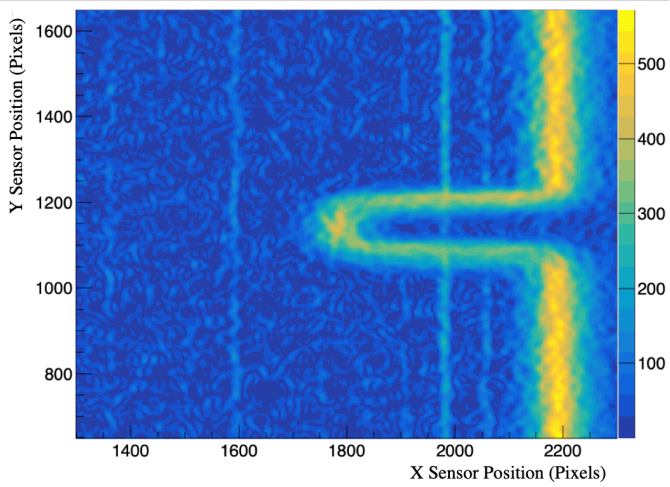

Fig. 8. Subsection of MLC leaf edge data frame at 20mm extension in radiotherapy treatment field, after applying the sobel operators.

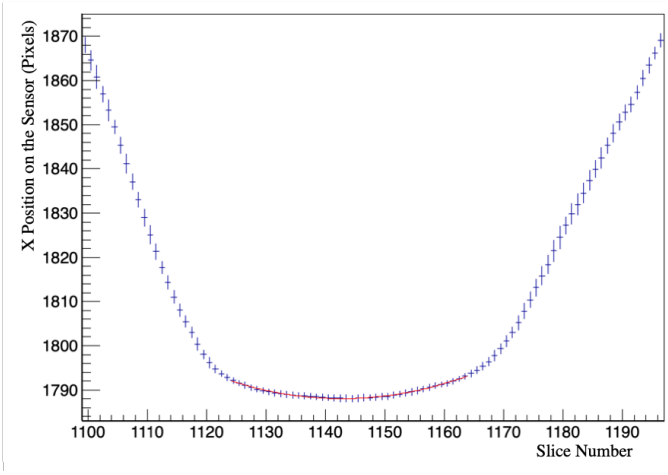

Fig. 9. Reconstructed leaf edge position for different slices through the MLC leaf. Please note that the actual leaf edge is not flat.

obtained in short time intervals. To determine the accuracy, the reconstructed leaf edge positions were plotted as a function of the set MLC position, see Fig. 12. Note that the reconstructed leaf position corresponds to the X position of the sensor as indicated in Fig. 4, which runs in the opposite direction to the set leaf position of the LINAC. The reconstructed X position in pixels was scaled by the 50 μm pixel pitch. The data was fit with a straight line. This yielded a slope of -1.00$\pm$0.01, which agrees well with 1. Hence, this technique returns the correct position over the entire range of leaf extensions studied in this work.

VIII. Conclusion

We are developing a MAPS based real time radiotherapy treatment verification device. A key task of such a system is to monitor the leaf positions in real time. Here we present results using the Lassena, a 12$\times$14 cm^2, three side buttable sensor. A 2$\times$2 matrix of these sensors covers a large enough area to be clinically deployed. Results for a single, central,

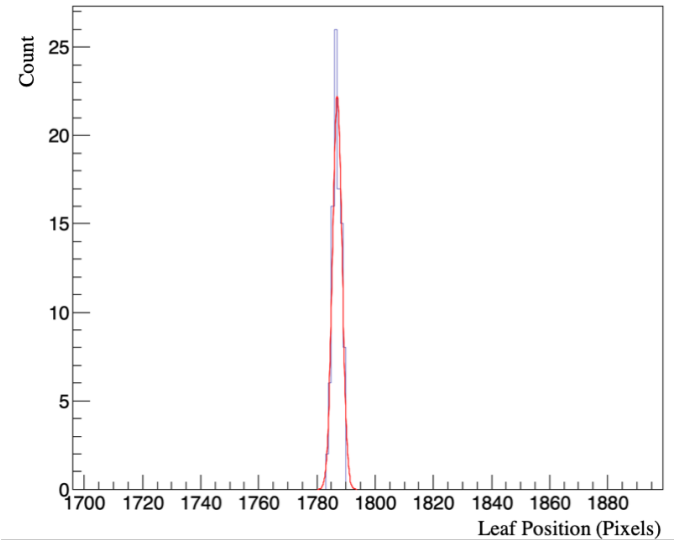

Fig. 10. Histogram of 90 individual measurements for the 20mm MLC leaf edge position. It can be seen that a Gaussian fit is applied. The sigma of this Gaussian is used to determine resolution. Similar histograms have been produced for all other set MLC positions.

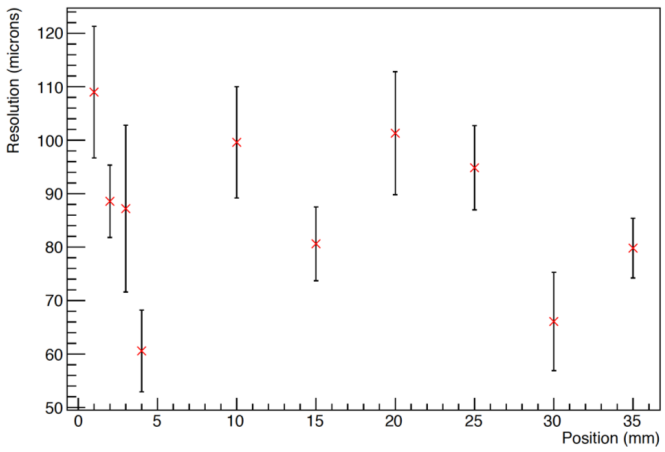

Fig. 11. Resolution calculated for each MLC position.

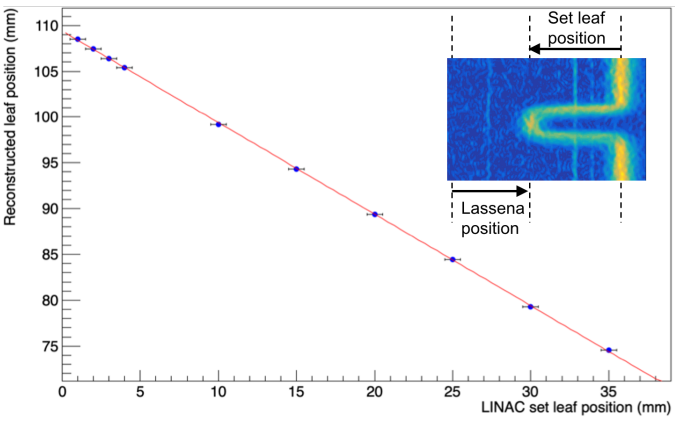

Fig. 12. Reconstructed MLC leaf edge position plotted as a function of the set leaf position as denoted by the LINAC. Note that the direction of the reconstructed leaf position with the Lassena is opposite to the direction of the LINAC set leaf extension.

MLC leaf at different extensions within a square radiotherapy treatment field have been reported. These results show that leaf positions can be reconstructed with resolutions between 60.6$\pm$7.65 μm and 109$\pm$12.3 μm at the isocentre in $\sim$0.3 s long treatment segments for a single, central, 5 mm thin leave using a 6 MV beam. This shows that excellent resolution is achieved throughout the treatment field. The MLC leaf edge resolutions are significantly better than current verification standards of $\pm$1 mm and the recommended verification standard of $\pm$0.3 mm previously described. This is true across the range of leaf positions and studied in this treatment field. It can be seen that the presence of other leaves can affect the reconstructed position, as observed in the leaf position measurements for a 1 mm extension. Detailed studies on leaf position resolutions for complex leaf configurations and leaves far away from the centre are ongoing. This is the first work that examines the leaf position precision in a large format MAPS, large enough for clinical deployment.

Radiation tolerance tests are in progress. Initial results show that the sensor is still fully operational after exposure to a radiation dose of 50 kGy administered with protons. In contrast to photons and electrons, protons also damage the epitaxial layer of the sensor and as such are a far more severe test of the radiation tolerance of the sensor. When deployed, this device could reduce total LINAC usage, including out-of-hours staff time, as pre-treatment verification would not be required. Treatments can also be verified to a higher precision than current standards. Errors, such as offset or stuck MLC leaf edges can also be identified instantaneously and treatment subsequently amended or halted immediately, hence increasing patient safety.

ACKNOWLEDGMENT

This research was funded by STFC through ST/S000143/1 and EPSRC through an EPSRC DTA studentship.

REFERENCES

[1] Public Health England, "Radiotherapy activity across England" 2017 [online]. Available at: http://www.ncin.org.uk/view?rid=3426

[2] Staffurth, J. (2010). A review of the clinical evidence for intensity-modulated radiotherapy. Clinical oncology, 22(8), 643-657.

[3] Baumann, M., Krause, M., Overgaard, J., Debus, J., Bentzen, S.M., Daartz, J., Richter, C., Zips, D. & Bortfeld, T. (2016). Radiation oncology in the era of precision medicine. Nature Reviews Cancer, 16(4), 234.

[4] Klein, E. E., Hanley, J., Bayouth, J., Yin, F. F., Simon, W., Dresser, S. & Liu, C. (2009). Task Group 142 report: Quality assurance of medical accelerators a. Medical physics, 36(9Part1), 4197-4212.

[5] Graves, M. N., Thompson, A. V., Martel, M. K., McShan, D. L., & Fraass, B. A. (2001). Calibration and quality assurance for rounded leafend MLC systems. Medical physics, 28(11), 2227-2233.

[6] Agarwal, A., Rastogi, N., Das, K. M., Yoganathan, S. A., Udayakumar, D., Naresh, R., & Kumar, S. (2019). Evaluating the dosimetric consequences of MLC leaf positioning errors in dynamic IMRT treatments. Journal of Radiotherapy in Practice, 1-7

[7] Stell, A. M., Li, J. G., Zeidan, O. A., & Dempsey, J. F. (2004). An extensive logfile analysis of stepandshoot intensity modulated radiation therapy segment delivery errors. Medical physics, 31(6), 1593-1602.

[8] Rangel, A., & Dunscombe, P. (2009). Tolerances on MLC leaf position accuracy for IMRT delivery with a dynamic MLC. Medical physics, 36(7), 3304-3309

[9] LoSasso, T., Chui, C. S., & Ling, C. C. (2001). Comprehensive quality assurance for the delivery of intensity modulated radiotherapy with a multileaf collimator used in the dynamic mode. Medical physics, 28(11), 2209-2219.

[10] Kutcher, G. J., Coia, L., Gillin, M., Hanson, W. F., Leibel, S., Morton, R. J. & Weller, M. (1994). Comprehensive QA for radiation oncology: report of AAPM radiation therapy committee task group 40. Medical physics, 21(4), 581-618.

[11] B. Poppe et al., Davida translucent multi-wire transmission ionization chamber for in vivo verification of imrt and conformal irradiation techniques, Phys. Med. Biol., vol. 51, no. 5, pp. 12371248, 2006.

[12] S. Venkataraman et al., The influence of a novel transmission detector on 6 mv x-ray beam characteristics, Phys. Med. Biol., vol. 54, no. 3173-83, 2009.

[13] Van Elmpt, W., McDermott, L., Nijsten, S., Wendling, M., Lambin, P., & Mijnheer, B. (2008). A literature review of electronic portal imaging for radiotherapy dosimetry. Radiotherapy and oncology, 88(3), 289-309.

[14] Baker, S. J., Budgell, G. J., & Mackay, R. I. (2005). Use of an amorphous silicon electronic portal imaging device for multileaf collimator quality control and calibration. Physics in Medicine & Biology, 50(7), 1377.

[15] Velthuis, J. J., Hugtenburg, R. P., Cussans, D., Perry, M., Hall, C., Stevens, P. & McKenzie, A. (2014). The VANILLA sensor as a beam monitoring device for X-ray radiation therapy. Applied Radiation and Isotopes, 83, 8-11.

[16] Velthuis, J., Hugtenburg, P. R., Hall, C., Page, R., & Stevens, P. Monitoring of a therapeutic X-ray beam using an active pixel sensor detector. Patent granted in EU on 04/04/2018, EP2654895B1.

[17] Velthuis, J., Hugtenburg, P. R., Hall, C., Page, R., & Stevens, P. (2016). Upstream direct x-ray detection. U.S. Patent No. 9,517,358. Washington, DC: U.S. Patent and Trademark Office.

[18] Beck, L., Velthuis, J. J., Fletcher, S., Haynes, J. A., & Page, R. F. (2020). Using a TRAPS upstream transmission detector to verify multileaf collimator positions during dynamic radiotherapy delivery. Applied Radiation and Isotopes, 156, 108951.

[19] Page, R.F., Abbott, N.L., Davies, J., Dyke, E.L., Randles, H.J., Velthuis, J.J., Fletcher, S., Gregory, S.D., Hall, C., John, A.M. and Lawrence, H., (2014). Using a monolithic active pixel sensor for monitoring multileaf collimator positions in intensity modulated radiotherapy. IEEE Transactions on Nuclear Science, 61(1), 74-78.

[20] J. H. Hubbell and S. M. Seltzer, Tables of x-ray mass attenuation coefficients and mass energy-absorption coefficients (version 1.4), National Institute of Standards and Technology, Gaithersburg, MD, USA, 2012. [Online]. Available: http://physics.nist.gov/xaamdi

[21] Fossum, E. R. (1993, July). Active pixel sensors: Are CCDs dinosaurs?. In Charge-Coupled Devices and Solid State Optical Sensors III (Vol. 1900, pp. 2-14). International Society for Optics and Photonics.

[22] Guerrini, N., Turchetta, R., Van Hoften, G., Henderson, R., McMullan, G., & Faruqi, A. R. (2011). A high frame rate, 16 million pixels, radiation hard CMOS sensor. Journal of Instrumentation, 6(03), C03003.

[23] Beck, L., Velthuis, J. J., Fletcher, S., Haynes, J. A., & Page, R. F. (2019). Using a TRAPS upstream transmission detector to verify multileaf collimator positions during dynamic radiotherapy delivery. Applied Radiation and Isotopes, 108951.

[24] Velthuis, J. J., Page, R. F., Hugtenburg, R. P., Blake, S. W., Crawford, D., Fletcher, S., Saunders, M., & Stevens, P. H. (2014). 207: An Intensity Modulated Radiotherapy Beam Monitoring System using a Monolithic Active Pixel Sensor. Radiotherapy and Oncology, 110, S101-S102.

[25] Sedgwick, I., Das, D., Guerrini, N., Marsh, B., & Turchetta, R. (2013). LASSENA: A 6.7 megapixel, 3-sides buttable wafer-scale CMOS sensor using a novel grid-addressing architecture. International Image Sensor Society.